ELSEVIER

Journal of Nuclear Materials 252 (1998) 228–234

journal of nuclear materials

Thermophysical property measurements and ion-implantation studies on $CePO_4$

K. Bakker [a,*], H. Hein [a], R.J.M. Konings [a], R.R. van der Laan [a], Hj. Matzke [b], P. van Vlaanderen [a]

[a] *Netherlands Energy Research Foundation ECN, P.O. Box 1, 1755 ZG Petten, The Netherlands*
[b] *European Commission, Joint Research Centre, Institute for Transuranium Elements, Postfach 2340, D-76125 Karlsruhe, Germany*

Received 11 August 1997; accepted 3 October 1997

Abstract

The thermal properties and the response to fission-product damage of $CePO_4$ were studied in view of its potential application as inert matrix for the transmutation of transuranium elements in nuclear reactors. The thermal expansion of $CePO_4$ has been recorded from 293 K to 1323 K using X-ray diffraction. The reduced enthalpy increment of $CePO_4$ has been measured by drop calorimetry from 474 K to 934 K. The laser-flash technique was used to measure the thermal diffusivity between 300 K and 1150 K. Ion implantation studies were performed at 813 K with 72 MeV ^{127}I ions and at room temperature with 403 MeV ^{116}Sn ions. The results are not favourable for the use of $CePO_4$ as inert matrix to incinerate actinides. © 1998 Elsevier Science B.V.

1. Introduction

The mineral monazite, a rare-earth phosphate, occurs as an accessory mineral in granitic rocks and is the principal source for the commercial production of cerium and other lanthanide elements. Monazite has the ability to incorporate large amounts of thorium and uranium and remains crystalline despite the high α-decay doses (>1 dpa, displacement per atom) induced by these elements. α-decay produces α-particles ($\simeq 5$ MeV, producing $\simeq 200$ displacements in the lattice). The recoil atoms of the α-decay, e.g. ^{237}Np in the decay of ^{241}Am, $\simeq 100$ keV, produce $\simeq 1500$ displacements in the lattice. For this reason synthetic monazite is being considered as a storage medium for transuranium elements like plutonium and americium [1–3].

The α-decay resistance and the ability to incorporate thorium and uranium make synthetic monazite ($CePO_4$) also an interesting support material for uranium-free fuels that are considered for the incineration of plutonium and americium, especially in once-through scenarios. While being reactor irradiated, monazite will experience the impact of fission products with 70 to 100 MeV energy, one fission event producing $\simeq 1\times10^5$ displacements. The range of fission products is $\simeq 8$ μm, compared to $\simeq 20$ μm for α-particles and $\simeq 0.03$ μm for recoil atoms. At present no information is available on the influence of irradiation with fission products on the microstructure of $CePO_4$. A useful technique to study fission damage is by using high-energy ion beams. This avoids the formation of radioactive species and the need to work in hot cells. The only information that exists about the influence of ions on the microstructure of $CePO_4$ has been obtained at energies that are much lower than the energies of fission products [4,5]. Monazite becomes metamict during irradiation with 1.5 MeV Kr ions at doses below 1 dpa [4]. Karioris et al. [5] have shown that monazite becomes also metamict when bombarded with Ar ions (3 MeV). It recrystallizes by annealing at approximately 570 K for 24 h. The stability against fission product impact at fission energy is studied in the present investigation.

* Corresponding author. Tel.: +31-224 564 386; fax: +31-224 563 608; e-mail: k.bakker@ecn.nl.

PII S0022-3115(97)00300-0

In addition to the influence of irradiation on the microstructure, the thermal properties of monazite are also of major importance for the applicability of monazite as a support material for uranium-free fuels. The thermal conductivity is one of the main thermal properties, since it influences directly the central temperature of the fuel. Since $CePO_4$ melts at 2318 ± 20 K [6], the thermal conductivity of $CePO_4$ must be relatively large in order to keep a safe margin between the central temperature and the melting point. Other properties that have been determined in the present study are the heat capacity, which is an important parameter for the safety analysis and the thermal expansion which is important for the design of the fuel.

2. Experimental

$CePO_4$ was prepared from $Ce_2(SO_4)_3 \cdot 9H_2O$, which was dissolved in water. This solution was added to a $NH_4H_2PO_4$ solution and after thoroughly stirring the pH of the solution was adjusted to 4. The ratio of $Ce_2(SO_4)_3 \cdot 9H_2O$ to $NH_4H_2PO_4$ that is thus obtained is approximately 0.1. The $CePO_4$ precipitate was filtered, dried at 400 K and heated in air at 1273 K. The powder obtained was pressed into pellets and sintered in air at 1873 K for 10 h. The densities of the thus obtained pellets showed a variation between 75% and 95% of the theoretical density, but this method is not reproducible. In the present study $CePO_4$ was therefore also produced using the procedure described by Hikichi and Nomura [6], using an aqueous solution of $CeCl_3 \cdot 7H_2O$ (0.05 mol dm^{-3}). The solution was rapidly added to a dilute H_3PO_4 solution (P/Ce mole ratio 20). After mixing the pH was adjusted to 1 using diluted NH_4OH. This mixture was stirred overnight and the $CePO_4$ precipitate was filtered and washed four times in water and two times in acetone and dried at 383 K. This powder was milled, heated in air at 1273 K, pressed into pellets, and sintered in air at 1873 K for 5 h. Using this technique pellets with a reproducible theoretical density between 85% and 90% were obtained.

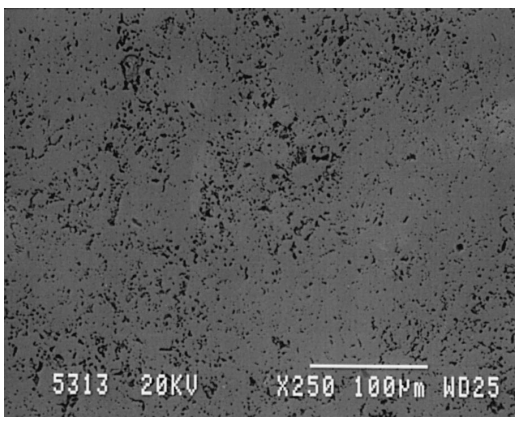

Fig. 1. Scanning electron microscopy image of a single-phase $CePO_4$ sample. The small dark areas are pores.

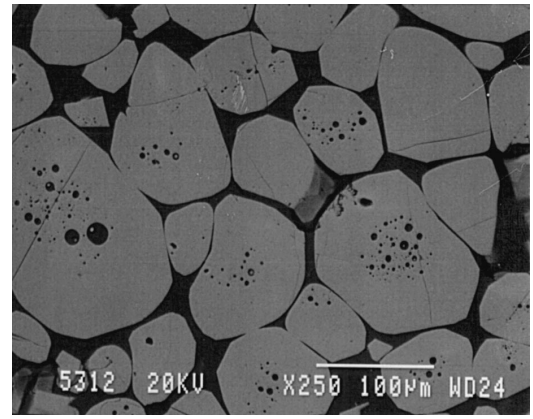

Fig. 2. Scanning electron microscopy image of a two-phase $CePO_4$ sample. The light areas are the $CePO_4$ phase, the dark areas are the CeP_3O_9 phase.

X-ray diffraction analysis did not reveal other phases in the $CePO_4$ samples. However, using optical microscopy it was observed that a small amount of second-phase material is present at the grain edges in some of the samples. Using EDX microanalysis the second phase material was identified as CeP_3O_9. The formation of the CeP_3O_9 phase is probably caused by the excess of $NH_4H_2PO_4$ in the solution during the preparation. Since the CeP_3O_9-phase is only present at the grain boundaries it is assumed that CeP_3O_9 has a lower melting point than $CePO_4$. In the samples with a relatively high density (85%–95%) the CeP_3O_9-phase is present, while in the low density (75%–85%) samples this phase is absent. From this observation it can be concluded that the CeP_3O_9-phase increases the

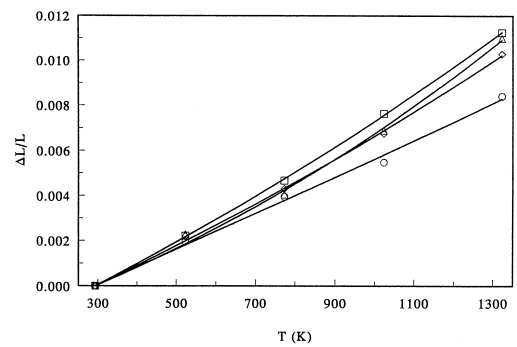

Fig. 3. Thermal expansion of $CePO_4$ for the three axes and for the volume/3. □ *c*-axis, △ *a*-axis, ◇ volume/3 and ○ *b*-axis. The lines represent fits (Eqs. (2)–(5)) through these data.

Table 1
Thermal expansion of $CePO_4$

T (K)	$\Delta a/a$(293 K)	$\Delta b/b$(293 K)	$\Delta c/c$(293 K)	$1/3\Delta V/V$(293 K)
523	2.27×10^{-3}	1.95×10^{-3}	2.21×10^{-3}	2.19×10^{-3}
773	4.06×10^{-3}	3.96×10^{-3}	4.67×10^{-3}	4.31×10^{-3}
1023	6.90×10^{-3}	5.48×10^{-3}	7.64×10^{-3}	6.76×10^{-3}
1323	10.99×10^{-3}	8.41×10^{-3}	11.25×10^{-3}	10.29×10^{-3}

density, probably by liquid phase sintering. The microstructures of two samples without and with the second phase, respectively, are shown in Figs. 1 and 2. In the present investigation only single-phase $CePO_4$ samples have been used, except for the ^{116}Sn ion implantation study. The sintered pellets are much softer and are more easily broken than most other ceramics.

Thermal expansion measurements were performed using X-ray diffraction in air with a Guinier–Lenné camera ($Cu\,K\alpha_{1,2}$ radiation), using α-SiO_2 as an external standard. Measurements were performed at room temperature, 523 K, 773 K, 1023 K, and 1323 K in sequential order, after which the sample was cooled down to room temperature and another measurement was performed.

The enthalpy increments were measured in an isothermal diphenyl-ether drop-calorimeter, as previously described by Cordfunke et al. [7]. For the experiment 5.53 g of $CePO_4$ was enclosed in a quartz capsule of 1.69 g.

The thermal diffusivity (d) was measured with the laser-flash technique. The thermal conductivity (λ) was derived combining the data on the thermal diffusivity, heat capacity (c_p) and the density (ρ):

$$\lambda = d\rho c_p. \quad (1)$$

Ion implantation studies of pellets of $CePO_4$ were performed at the

· TASCC accelerator, Chalk River, AECL, Canada (cooperation with R.A. Verrall and P.G. Lucuta) using a beam of an element occurring in fission with its proper fission energy, i.e. ^{127}I at 72 MeV, and the

· GANIL accelerator, Caen, France (cooperation with M. Toulemonde) using a beam of ^{116}Sn at the very high energy of 403 MeV.

3. Thermal properties

3.1. Thermal expansion

$CePO_4$ has a monoclinic crystal structure in which the following room temperature lattice parameters have been obtained in the present study: $a = 0.67971(9)$ nm, $b = 0.70239(8)$ nm, $c = 0.64739(11)$ nm and $\beta = 103.47°$. The variation of β in the temperature range from 293 K to 1323 K was found to be smaller than our experimental inaccuracy ($< 0.04°$). The room temperature results are in good agreement with the data of Uedo [8], who observed: $a = 0.68004(11)$ nm, $b = 0.70231(13)$ nm, $c = 0.64717(10)$ nm and $\beta = 103.46°$.

The changes of the lattice parameters a, b, c, and of a third of the volume are shown in Fig. 3 and in Table 1.

Table 2
Enthalpy increments of $CePO_4$

T (K)	$\{H^0(T) - H^0(298.15\ K)\}$ (J mol^{-1})		δ (%)
	experimental	calculated	
474.1	20674	20752	−0.38
499.4	24081	24010	0.30
525.0	27352	27356	−0.01
576.1	34136	34175	−0.11
627.1	41210	41148	0.15
678.4	48443	48317	0.26
729.1	55379	55542	−0.29
780.8	62966	63046	−0.13
831.1	70641	70473	0.24
883.0	78162	78263	−0.13
933.7	86025	85991	0.04

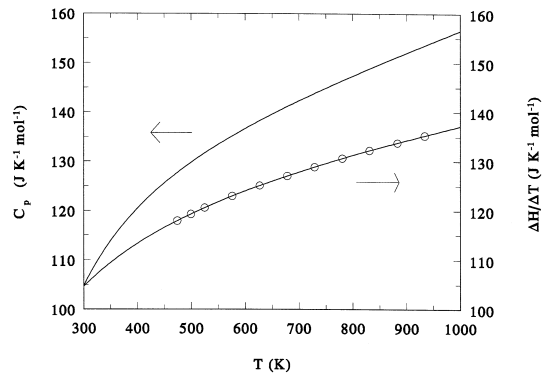

Fig. 4. The measured and the fitted reduced enthalpy increment data and the heat-capacity curve of $CePO_4$.

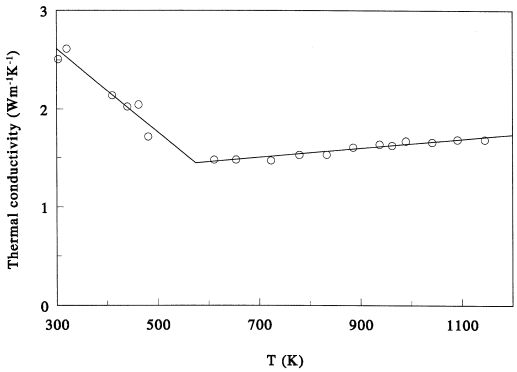

Fig. 5. Thermal conductivity of fully dense $CePO_4$. The lines represent Eqs. (10) and (11).

The following equations represent the results:

$$\Delta a/a(293\ \mathrm{K}) = 7.32\times10^{-6}\times(T-293) + 3.18\times10^{-9}\times(T-293)^2.$$

$$\Delta b/b(293\ \mathrm{K}) = 7.77\times10^{-6}\times(T-293) + 2.72\times10^{-10}\times(T-293)^2.$$

$$\Delta c/c(293\ \mathrm{K}) = 9.00\times10^{-6}\times(T-293) + 1.88\times10^{-9}\times(T-293)^2.$$

$$1/3\Delta V/V(293\ \mathrm{K}) = 8.25\times10^{-6}\times(T-293) + 1.63\times10^{-9}\times(T-293)^2.$$

The measured values of the lattice parameters after the thermal expansion measurement show a slight increase ($\simeq 5\times10^{-13}$ m), compared to the initially measured lattice parameters, which is due to the experimental setup of the X-ray equipment. To derive Eqs. (2)–(5) only the initial room temperature measurement has been used. The error in the thermal expansion data, which is approximately 10%, has been deduced by comparing the measured lattice parameters before and after the thermal expansion measurement.

Table 3
Thermal diffusivity d and thermal conductivity λ of 100% dense $CePO_4$

T (K)	d (mm^2 s^{-1})	λ (W m^{-1} K^{-1})
303	1.073	2.51
320	1.084	2.62
410	0.797	2.14
440	0.736	2.03
462	0.732	2.05
481	0.607	1.72
611	0.491	1.48
654	0.483	1.48
723	0.468	1.47
779	0.478	1.53
833	0.471	1.53
885	0.487	1.61
937	0.490	1.64
962	0.483	1.63
989	0.493	1.67
1041	0.483	1.66
1091	0.485	1.69
1145	0.479	1.69

The thermal expansion of the *b*-axis is smaller than that of both the *a* and the *c*-axis. Hikichi et al. [9] determined the linear thermal expansion coefficient (α) of approximately 99% dense $CePO_4$ ceramics using a dilatometer. They reported: $\alpha(298\ \mathrm{K}) = 9\times10^{-6}\ \mathrm{K}^{-1}$, $\alpha(773\ \mathrm{K}) = 10\times10^{-6}\ \mathrm{K}^{-1}$ and $\alpha(1573\ \mathrm{K}) = 11\times10^{-6}\ \mathrm{K}^{-1}$. Our data suggest a slightly stronger temperature dependence of the linear thermal expansion.

3.2. Enthalpy increment

The results of the drop caloric measurements for $CePO_4$ are listed in Table 2. The results have been fitted to the polynomial

$$H^0(T) - H^0(298.15\ \mathrm{K})\ (\mathrm{J\ mol^{-1}}) = 119.95796\times T + 1.9490197\times10^{-2}\times T^2 + 2.412137\times10^6\times T^{-1} - 45588.4 \quad (6)$$

applying $H^0(T) - H^0(298.15\ \mathrm{K}) = 0$ at 298.15 K as

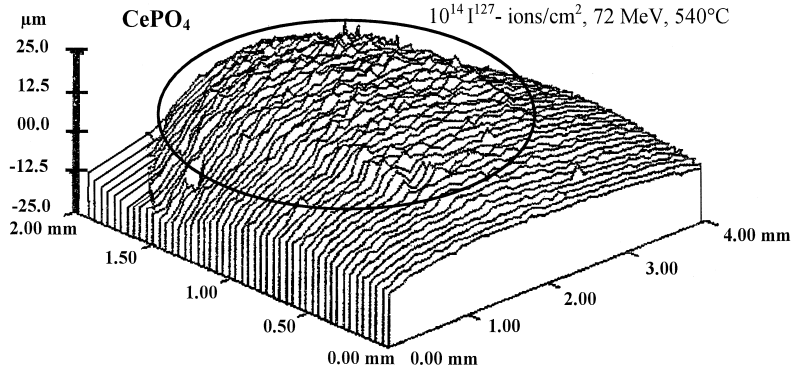

Fig. 6. Laser scan of $CePO_4$ irradiated with 1×10^{14} ^{127}I ions cm^{-2} of 72 MeV energy at 813 K showing the large swelling of the irradiated spot.

boundary condition. The heat capacity is the derivative of the enthalpy increment

$$C_p\,(\mathrm{J\,K^{-1}\,mol^{-1}}) = 119.958 + 3.898 \times 10^{-2} \times T - 2.412 \times 10^{6} \times T^{-2}. \quad (7)$$

Both equations are accurate within 1% in the temperature range between 474 K and 934 K. Extrapolation of Eq. (7) yields a heat capacity of 104.446 J K^{-1} mol^{-1} at 298.15 K. The measured and the fitted reduced enthalpy increment data ($\{H^0(T) - H^0(298.15\ \mathrm{K})\}/(T - 298.15\ \mathrm{K})$) and the heat-capacity curve are shown in Fig. 4.

The heat capacity of $CePO_4$, expressed per unit of volume, is nearly identical to that of UO_2. Hikichi et al. [9] determined the heat capacity at 298 K (101.1 J K^{-1} mol^{-1}) and at 773 K (138.7 J K^{-1} mol^{-1}). Their result at 298 K is 4% lower than our extrapolated heat-capacity curve and their measurement at 773 K is 5% lower than our curve. Hence, reasonable agreement is observed.

A differential thermal analysis experiment has been performed between room temperature and 1973 K using a

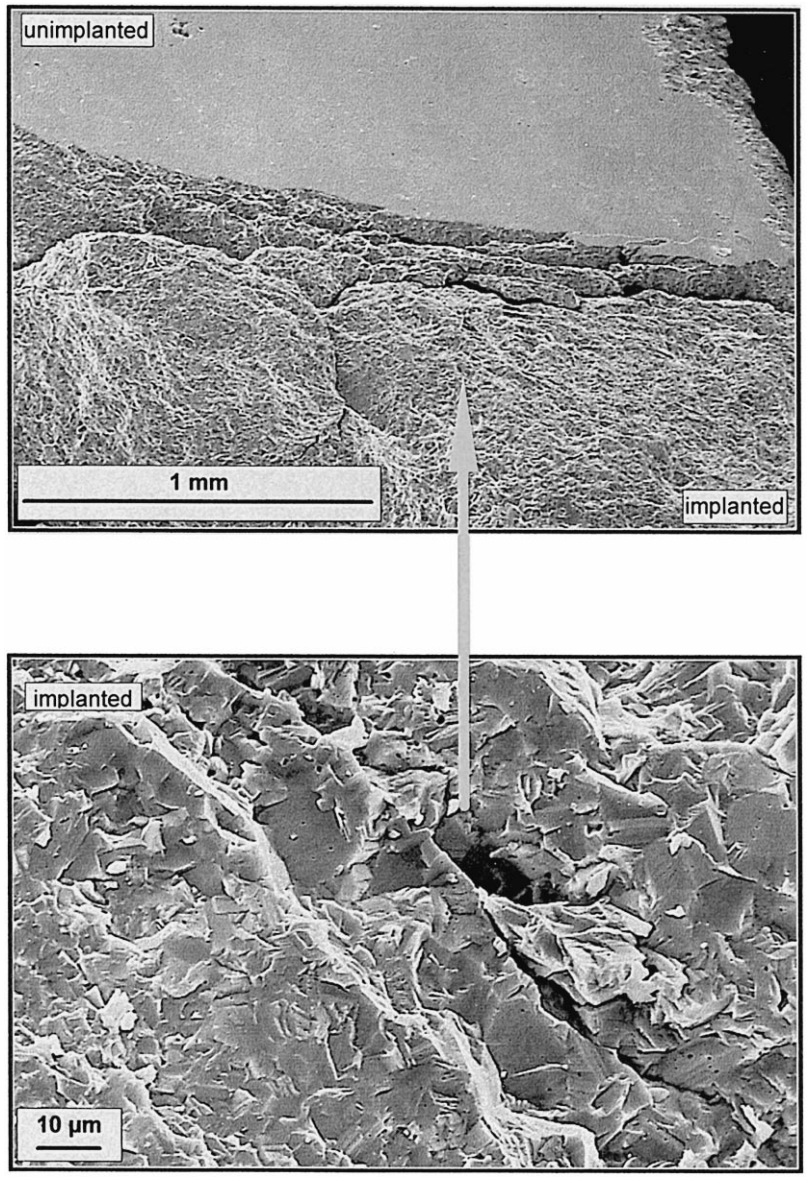

Fig. 7. Scanning electron microscopy image of $CePO_4$ irradiated with 3.2×10^{13} ^{116}Sn ions cm^{-2} of 403 MeV energy at room temperature. The upper part shows the edge of the beam spot, the lower part shows details of the irradiated area.

Bähr thermoanalyse DTA typ 701. No transitions have been observed in $CePO_4$ in this temperature range.

3.3. Thermal diffusivity and thermal conductivity

The thermal diffusivity has been measured by the laser flash technique, using a $CePO_4$ sample with a density of 80.2% th.d. From these data the thermal conductivity (Fig. 5 and Table 3) has been obtained using the heat capacity data and the density (corrected for thermal expansion) described in the previous sections. The measurements were corrected to a density of 100% using Eq. (8), that describes the influence of randomly ordered spherical porosity on the thermal conductivity [10]

$$f = (1 - p)^{1.5}, \tag{8}$$

where p is the porosity and f is the heat flow in the porous material divided by that in fully dense material.

In the temperature range presently investigated the thermal conductivity of most ceramic oxides is governed by the phonon contribution which is described by

$$\lambda = 1/(A + BT). \tag{9}$$

Only below 500 K the $CePO_4$ data can be described by Eq. (9). Various effects might cause the deviation from Eq. (9) for temperatures above 600 K, such as: (i) an electronic contribution to the thermal conductivity [11], or (ii) the thermal conductivity becomes constant since the phonon mean free path has reached its lower limit [12].

The following equations are fits through the data:

$$\lambda(\mathrm{W\ m^{-1}\ K^{-1}}) = 3.89 - 4.27 \times 10^{-3} \times T \quad (300\ \mathrm{K} \le T \le 574\ \mathrm{K}), \tag{10}$$

$$\lambda(\mathrm{W\ m^{-1}\ K^{-1}}) = 1.17 + 4.73 \times 10^{-4} \times T \quad (574\ \mathrm{K} < T \le 1150\ \mathrm{K}). \tag{11}$$

These fits are made in order to simplify the application of the data. It is not claimed that at 574 K a sharp kink exists in the thermal conductivity. The inaccuracy of the thermal conductivity data is approximately 15%, which is mainly induced by the thermal diffusivity data and the porosity correction. The thermal conductivity of approximately 99% dense $CePO_4$ as determined by Hikichi et al. [9] at two temperatures is: $\lambda(298\ \mathrm{K}) = 3.08\ \mathrm{W\ m^{-1}\ K^{-1}}$ and $\lambda(773\ \mathrm{K}) = 1.81\ \mathrm{W\ m^{-1}\ K^{-1}}$. These two values are both approximately 20% higher than our values.

4. Ion implantation studies

Typical results of ion implantation studies are shown in Figs. 6 and 7. Fig. 6 is a laser scan of the implanted surface, which shows that the swelling of $CePO_4$ is very large under fission product impact, even at low doses and at elevated temperature. The implanted spot 'pops out' due to the unilateral swelling, as has been observed before on e.g. Al_2O_3 [13]. This swelling is of the order of 20% though the damage produced corresponds to that of a very short irradiation of $< 0.1\%$ FIMA only. The state of the swollen material (crystalline or amorphous, original grains or polygonized) has not been analyzed yet. It is planned to apply transmission electron microscopy to determine the microstructure. A similar poor irradiation stability of $CePO_4$ was observed during irradiation with 1.5 MeV Kr ions [4] and 3 MeV Ar ions [5]. Fig. 7 shows the consequences of the impact of ions with high energy. The implanted area is seen to be fractured and part of the fracture pieces has been expelled by the ion impact, the mechanism probably being Coulomb explosion.

5. Discussion

The thermal conductivity of $CePO_4$ is relatively small compared to that of nuclear fuels (e.g. UO_2) or other potential inert matrix materials (e.g. $MgAl_2O_4$, $Y_3Al_5O_{12}$). The combination of a low thermal conductivity and the low melting point (2318 ± 20 K) [6] is very unfavourable, since it limits the maximum allowable power generated during reactor operation. Low power operation of the fuel decreases the transmutation rate and has an unfavourable influence on the economics of the transmutation process.

In order to analyse the influence of the low thermal conductivity a radial temperature profile in a $CePO_4$ transmutation fuel pellet contained in a fuel rod has been computed (Fig. 8) using the following conditions and conservative assumptions:

- The thermal conductivity of a mixture of $CePO_4$ with actinide oxides is identical to that of $CePO_4$, and the thermal conductivity is not influenced by irradiation.
- The thermal conductivity of $CePO_4$, as determined in the temperature range between 574 K and 1150 K (Eq. (11)), can be extrapolated to 1800 K.
- The power generated in the fuel is 22 kW m^{-1} and the power density along the radius of the fuel is constant.

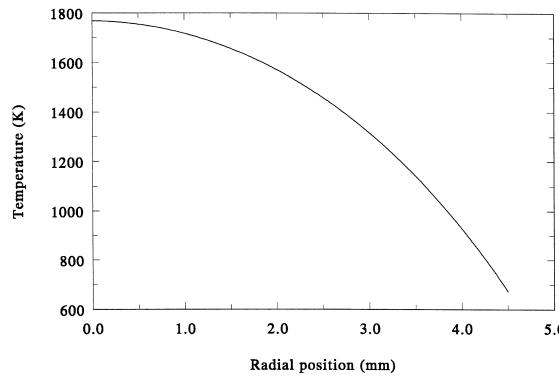

Fig. 8. Radial temperature distribution in a $CePO_4$ pellet in which a power of 22 kW m^{-1} is generated.

· The diameter of the $CePO_4$ pellet is 9.0 mm, the density of the pellet is 95% th.d. and the outer temperature of the pellet is 673 K.

At the relatively low power of 22 kW m^{-1} the central fuel temperature is only $\simeq 540$ K lower than the melting temperature of $CePO_4$. This temperature difference is insufficient for safe operation of the fuel. Fig. 8 gives only a rough estimation of the temperature profile in the fuel due to the extrapolation of the thermal conductivity over a large temperature range and due to the fact that the influence of irradiation on the thermal conductivity is unknown. It is likely that the thermal conductivity of $CePO_4$ will be strongly reduced by the irradiation induced swelling and by defect formation and that the central temperature will increase even further.

The radiation stability against fission damage and impact of high energy ions of the $CePO_4$ used in this study is very poor. Especially the impact of the 72 MeV ^{127}I ions on the $CePO_4$ sample at 813 K is of importance since these conditions are fairly comparable to the conditions experienced by $CePO_4$ when it serves as a support material for transmutation. The main difference between these two conditions is the irradiation rate. This difference amounts to about three orders of magnitude. No information exists on dose rate effects in $CePO_4$. Information is available for UO_2, and the existing evidence does not show significant dose rate effects [13].

The results suggest that the stability of $CePO_4$ towards α-decay is different from that towards ion implantation, which seems to indicate a dose rate effect. However, the energy-loss conditions of the damaging ions and the defect cascades formed in fission and in α-decay are vastly different. These two different damage sources should therefore not be directly compared.

6. Conclusion

Because of the rather low thermal conductivity in combination with the relatively low melting point together with the poor radiation stability against high energy heavy ions (simulating fission product damage), it is concluded that cerium phosphate is not a suitable inert matrix material. Our results do, however, not imply that monazite is not a good matrix to embed actinides for long time storage.

Acknowledgements

The authors would like to thank P.G. Lucuta and R.A. Verrall (Chalk River, AECL) and M. Toulemonde (GANIL, Caen) for help with the high energy ion implantations. R.A. Verrall provided also the laser scan on Fig. 6. Thanks are also due to T. Wiss (ITU) for the SEM observations.

References

[1] R.R. Parrish, Can. J. Earth Sci. 27 (1990) 1431.
[2] L.A. Boatner, G.W. Beall, M.M. Abraham, C.B. Finch, P.G. Huray, M. Rappaz, in: C.J.M. Northrup, Jr. (Ed.), Scientific Basis for Nuclear Waste Management, vol. 2, Plenum, New York, 1980, p. 289.
[3] L.A. Boatner, M.M. Abraham, M. Rappaz, in: J.G. Moore (Ed.), Scientific Basis for Nuclear Waste Management, vol. 3, Plenum, New York, 1980, p. 181.
[4] A. Meldrum, L.M. Wang, R. Ewing, Nucl. Instrum. Meth. B 116 (1996) 220.
[5] F.G. Karioris, L. Cartz, K.A. Gowda, Radiat. Eff. Lett. 58 (1981) 1.
[6] Y. Hikichi, T. Nomura, J. Am. Ceram. Soc. 70 (1987) C–252.
[7] E.H.P. Cordfunke, R.P. Muis, G. Prins, J. Chem. Thermodyn. 11 (1979) 819.
[8] T. Uedo, J. Jpn. Assoc. Mineral. Petrol. Econ. Geol. 58 (1967) 170.
[9] Y. Hikichi, T. Nomura, Y. Tanimura, S. Suzuki, J. Am. Ceram. Soc. 73 (1990) 3594.
[10] B. Schulz, High Temp.–High Press. 13 (1981) 649.
[11] J.H. Harding, D.G. Martin, J. Nucl. Mater. 166 (1989) 223.
[12] G.A. Slack, Solid State Physics: Advances in Research and Applications, vol. 34, Academic Press, New York, 1979.
[13] Hj. Matzke, Nucl. Instrum. Meth. B 116 (1996) 121.